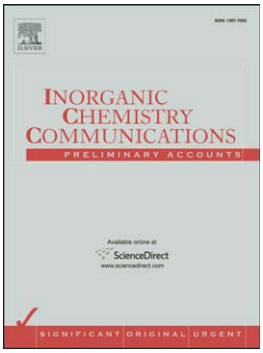

Studies on nucleic acid/protein interaction, molecular docking and antimicrobial properties of mononuclear nickel(II) complexes of piperazine based Schiff base

Arumugam Jayamani, Nallathambi Sengottuvelan, Sung Kwon Kang, Young-Inn Kim

PII: S1387-7003(14)00376-1
DOI: doi: 10.1016/j.inoche.2014.08.029
Reference: INOCHE 5716

To appear in: *Inorganic Chemistry Communications*

Received date: 5 August 2014
Accepted date: 28 August 2014

Please cite this article as: Arumugam Jayamani, Nallathambi Sengottuvelan, Sung Kwon Kang, Young-Inn Kim, Studies on nucleic acid/protein interaction, molecular docking and antimicrobial properties of mononuclear nickel(II) complexes of piperazine based Schiff base, *Inorganic Chemistry Communications* (2014), doi: 10.1016/j.inoche.2014.08.029

Studies on nucleic acid/protein interaction, molecular docking and antimicrobial properties of mononuclear nickel(II) complexes of piperazine based Schiff base

Arumugam Jayamani[a], Nallathambi Sengottuvelan[b]*, Sung Kwon Kang[c], Young-Inn Kim[d]

[a]*Department of Industrial Chemistry,* [b]*DDE, Alagappa University, Karaikudi -3*

[c]*Department of Chemistry, Chungnam National University, Daejeon 305-764, Korea*

[d]*Department of Chemistry Education and Interdisciplinary Program of Advanced Information and Display Materials, Pusan National University, Pusan 609-735, Korea*

*Corresponding author. Tel. /fax: +91 9488260744.

E-mail address: nsvelan1975@yahoo.com (N. SENGOTTUVELAN).

Abstract

The mononuclear nickel(II) complexes (**1**–**3**) of ligands bappz [1,4-bis(3-aminomethyl)piperazine] and its Schiff bases L^1 with 5-methyl salicylaldehyde; and L^2 with 5-bromosalicylaldehyde have been synthesized and characterized. The single crystal X-ray study showed that the complex **1** crystallized in the orthorhombic Pbca space group with distorted square planar geometry. The ligands and their nickel(II) complexes presented good binding propensity to bovine serum albumin protein (BSA). The strong binding interaction of the prepared complexes with calf thymus DNA (CT-DNA) was confirmed by absorption, fluorescence, circular dichroism spectral analysis and molecular docking studies in the order as follows: **3** > **2** > **1**. The Schiff bases and their Ni(II) complexes were also screened for antimicrobial activity. All the complexes exhibited higher antimicrobial activity than free ligands.

Keywords: Schiff base ligands; Antimicrobial activity; Nickel(II) complexes; DNA binding studies; Electrochemical studies.

Continued interest on the development of DNA binding agents has been driven by the goals for obtaining novel antitumor drugs, DNA sequencing agents and DNA conformation probes [1]. The interaction of drugs and their compounds with blood plasma proteins especially with serum albumin has involved in the transport of metal ions and metal complexes of drugs through the blood stream, is of increasing interest. Nickel is an important transition metal and its coordination compounds display interesting binding properties with proteins and nucleic acids [2]. The N- and O- containing ligands and their nickel(II) complexes have become important due to their wide biological activity anti-HIV activities etc. Bappz ligand molecule provides two pendant aminopropyl arms and two tertiary amines incorporated in the six-membered piperazine ring, which induces some sort of strain especially in the middle chelate ring when the two N-donor atoms of piperazine bind with Ni^{2+} ion [3]. Schiff bases derived from the salicyaldehyde and its derivatives are well known as polydentate ligands, coordinating in deprotonated or neutral forms. Schiff base complexes possess suitable biometric properties that can mimic the active sites and hence they have wide applications in as illness treatment, biochemical reactions and also as biological regulators [4].

Recently our research group reported that the mononuclear copper(II) complexes using Schiff base ligands L^1 [N, N′-bis(2-hydroxy-5-methylbenzyl)-1,4-bis(3-iminopropyl) piperazine] and L^2 [N, N′-bis(2-hydroxy-5-bromobenzyl)-1,4-bis(3-iminopropyl)piperazine] have molecular motion between N_4 and N_2O_2 compartments on varying pH and have good DNA interaction properties [5]. In order to study the change in molecular motion and DNA binding properties due to nickel(II) atoms, in this paper we have reported the synthesis (Scheme 1) of mononuclear nickel(II) complexes (**$[Ni(bappz)](ClO_4)_2$** [6], **$[NiL^1](ClO_4)_2$** [7]

and **$[NiL^2](ClO_4)_2$** [8]) of ligands bappz, Schiff bases L^1 and L^2 (Scheme 1), respectively were synthesized and characterized by elemental analysis, IR, UV-visible, ESI-Mass spectroscopy. The preparation of ligands and their crystal structure were reported in our previous work [5].

The X ray crystallographic analysis [9] of complex **1** (ORTEP diagram with 30% thermal probability ellipsoids shown in Figure 1, crystallographic data are listed in Table 1 and selected bond angle and bond distances are given in Table S1) shows that, the structure of the complex $[Ni(bappz)](ClO_4)_2$ (**1**) consists of monomeric isolated $[Ni^{II}(bappz)]^{2+}$ cations and two perchlorate counter anions in which one of the carbon atoms (C13) is disordered over two positions with an occupancy ratio of 0.62 (2) : 0.38 (2). The sum of the different angles around the Ni atoms is 359.98° indicating slightly distorted square-planar geometry around the metal atom. The distortion may conveniently be measured by the trans angles that are ideally 180° for a square-planar complex and 109.5° in a tetrahedral complex. The average N–M–N angles for the present Ni^{II} (173.9°) complex are larger than those for already the reported Cu^{II} (165.6°) complex with the same ligand [10]. The Ni–N(2) and Ni–N(15) distances (average 1.913 Å) are shorter than the Ni–N(6) and Ni–N(9) distances (average 1.930 Å) are mainly due to the different states of hybridization of nitrogen atom and/or the ring strain [11] due to boat conformation of inner piperazine unit. The non-coordinating perchlorate anions have a distorted tetrahedral structure, as indicated from their bond angles. In cif check report, the low ratio (43%) of the Ratio of Observed to Unique Reflections might be from the poor crystallinity of the complex.

The intermolecular Ni···Ni separation is 7.547 (2) Å, a value which does not permit any kind of bridging between the nickel atoms. Figure S1 shows the packing of the molecule in a lattice, which is stabilized by the H-bonding interactions between the oxygen of the anion with the piperazine ring hydrogen. The intramolecular hydrogen bonds are also

observed between the amino groups and nearer perchlorate O atoms (2.267 Å), which help in stabilizing the crystal structure.

The FT-IR spectrum of nickel(II) complexes (**2** and **3**) showed the broad peak at 3423–3450 cm^{-1} is assigned to the phenolic ν(OH) group [12]. The ligands and complexes showed a sharp band in the region of 1620–1650 cm^{-1} due to the presence of ν(C=N) [13]. The effective Schiff base condensation was confirmed by the disappearance of the ν(C=O) peak at 1680 cm^{-1}. All nickel(II) complexes showed a strong band around 1000–1100 cm^{-1} and a sharp band in the region around 625 cm^{-1} is due to the antisymmetric stretch and antisymmetric bend of the perchlorate ions respectively [14].

The absorption spectral data for Schiff base ligands and their complexes in DMF solution shows the peaks in the UV region of 270 nm to 278 nm are obtained due to $\pi \rightarrow \pi^*$ transition of coordinated ligands, broad and slightly intense bands between 384 and 396 nm due to ligand–metal charge transfer associated with the nitrogen and oxygen donors [15]. The visible spectra display the absorption bands below 670 nm assigned to the spin allowed d-d transitions, which have a low-spin d^8 nickel(II) ion in a square-planar environment [16].

Electron spray ionization (ESI) mass data of complex **2** (Figure S2) shows the molecular ion peak at *m/z* 694.2 (5), which is assignable to $[NiL^1+2ClO_4]^+$ and the loss of perchlorate ions as perchloric acid forms a base peak at *m/z* 493.3(100) due to the formation of $[NiL^1]^+$. In addition, few other intense peaks are obtained for **2** at *m/z* 375.3, 318.3 and 247.3. The ESI mass spectral data of the Schiff base nickel(II) complexes are in good agreement with the proposed structure of mononuclear nickel(II) complexes.

The solution of 0.05 M mononuclear nickel(II) complexes (**2** and **3**) in sodium perchlorate were acidified to pH 2 and titrated against standard NaOH solution. Titration with base induces colour change of the solution from brown to green and also result in the considerable change in absorption spectrum, as shown in Figure 2. In complex **2**, the strong

band at 337 nm (ε = 2836 M^{-1} cm^{-1}) decreases, while a new band develops at 389 nm (ε = 4047 M^{-1} cm^{-1}, limit value at pH 12). In the case of complex **3**, the strong band at 338 nm (ε = 2567 M^{-1} cm^{-1}) decreases, while a new band develops at 390 nm (ε = 3489 M^{-1} cm^{-1}, limit value at pH 12). The increase in absorbance (inset of Figure 3a and 3b) in d-d band and blue shift of absorption band upon changing the pH (acidic to basic) of the mononuclear nickel(II) complexes indicate that the colour and spectral changes are associated to the deprotonation process and thus the molecular motion i.e. the change of the position of nickel atom from N_4 compartment to N_2O_2 compartment is achieved by varying the pH of the complex solution [5].

The electrochemical behaviour of the nickel(II) complexes have been studied using cyclic voltammetry in the potential range from -1.80 V to +1.80 V in DMF containing 10^{-1} M tetra(n-butyl)ammonium perchlorate (with scan rate 50 mV s^{-1}). The complex exhibits redox wave on both the positive and the negative potential sides, corresponding to one electron oxidation and reduction, respectively (Figure S3). The cyclic voltammograms of complexes (**1**–**3**) show an irreversible reduction wave in negative potentials at -1.33V for **1**, -1.30V for **2**, and -1.17V for **3** correspond to Ni(II)—Ni(I) reduction. The corresponding reversible oxidation potential for Ni(II)—Ni(III) at 1.24V is observed for **1** and irreversible oxidation potential for Ni(II)—Ni(III) at 1.19V for **2** and 0.98V for **3**. The reduction and oxidation potential for nickel complexes of L^2 is observed at lower potential than L^1 complex due to the electron-withdrawing [17] substituent (Br) at the para position of the phenoxide oxygen in the phenyl ring of complex **3** [18].

Addition of ligands or its nickel(II) complexes **1**–**3** (dissolved in DMF) to BSA results in fluorescence quenching (up to 15% of the initial fluorescence intensity of BSA for bappz, 57% for $\mathbf{L^1}$, 64% for $\mathbf{L^2}$, 18% for **1**, 68% for **2**, 69% for **3**) (Figure 3), due to the possible

changes in secondary structure of BSA indicating the binding of the compounds to BSA [19]. According to Stern-Volmer quenching equation [20]:

$$I_0/I = 1+k_q\tau_0[Q] = 1 + K_{SV}[Q]$$

$$K_{SV} = k_q\tau_0$$

The calculated values of K_{sv} and k_q for the interaction of the compounds with the BSA are given in Table 2 and indicate a good BSA binding propensity of the compounds with bappz and its Schiff base complexes, out of which the complex **3** exhibiting the highest BSA quenching ability. Using the Scatchard equation [21]:

$$(\Delta I/I_0)/[Q] = nK- K(\Delta I/I_0)$$

It is obvious (Table 2) that the coordination of L^2 to Ni(II) results in an increased K value for BSA with complex **4** exhibiting the highest K value among the other complexes. The n values of ligands and complexes vary with slight increase or decrease when coordinated to Ni(II) in complexes **1–3** (Table 2) depending upon the availability of binding sites per albumin.

Absorption titration experiments were performed with fixed concentrations of the nickel(II) complexes (40 μM) while gradually increasing the concentration of DNA (0–10 mM) at 25 ^{o}C. On addition of increasing amounts of DNA to the complexes **1–3**, peak at 260 nm gradually increased with the hyperchromicity 60% for **1**, hyperchromicity of 40% for **2** and hypochromicity of 36% for **3** suggesting the strong interaction between complex and DNA. The isobestic point near 250 nm also proved the formation of the new complex between DNA and complex. The spectrophotometric titration of the complex **3** is shown in Figure 4 and other complexes are displayed in Figure S4. To compare quantitatively the binding strength of all the nickel(II) complexes, the intrinsic binding constants K_b of all the complexes with CT-DNA are determined according to the following equation [22]:

$$[DNA]/(\varepsilon_a - \varepsilon_f) = [DNA]/(\varepsilon_b - \varepsilon_f) + 1/K_b\ (\varepsilon_b - \varepsilon_f)$$

The K_b values obtained from the absorption spectral technique for the complexes **1**–**3** were calculated as 1.63 (2) × 10^5, 3.46 (2) × 10^5 and 6.44 (2) × 10^5 M^{-1} respectively, which is relevant to that of other typical groove binders and intercalators. The binding constants of the nickel(II) complexes of bappz and L^1 are relatively lower than that of the nickel(II) complex of L^2, which may be due to the presence of electron-withdrawing group (Br) in L^2 [23].

The emission spectrum of EB bound to DNA in the absence and presence of complex **3** is shown in Figure 5 and other complexes are displayed in Figure S5. The intensity of the emission band at 596 nm of the DNA–EB system decreased (up to 90.12% of the initial EB–DNA fluorescence intensity for **1**, up to 93.48% for **2**, up to 89.05% for **3**) upon addition of each complex **1**–**3** at diverse r values (Figure 5a) showing that each Ni(II) complex competes with EB to bind with DNA. The K_{SV} values of complexes (**1–3**) are calculated as 3.8 (3) × 10^5 M^{-1}, 5.5 (2) × 10^5 M^{-1} and 6.72 (3) × 10^5 M^{-1} respectively and vary in the order: **3** > **2** > **1**. The K_{SV} values illustrate that, the intercalary ability of Ni(II) complex of L^2 ligand has a better effect than L^1 complex. As the quenching of fluorescence is too low the apparent DNA binding constant (K_{app}) of the nickel(II) complexes **1–3** cannot be determined. The presence of 5-methyl (or bromo) salicylaldehyde groups and also the hydrophobic property of the rigid ligand facilitate the DNA binding [24].

The conformational changes in the UV region of CT-DNA induced by the complexes (**1**–**3**) were monitored by CD spectroscopy in buffer at room temperature, which show a distinct change in the spectral band corresponding to the B-DNA conformation (Figure 6). The nickel(II) complexes **1** and **2** exhibit groove binding interaction with large increase in intensity of the DNA helicity, in its positive as well as negative band with a higher red-shift. In complex **3** the ellipticity of the long wavelength positive band decreased in ellipticity of the interaction progressed with a slight red shift in the wavelength maximum and moderate changes also observed in the negative CD band at 245 nm indicates that intercalative

interaction involved in binding process. The binding between nickel(II) complexes and CT-DNA is due to the aromatic structure of ligands that provides planarity to the molecule. Moreover, in terms of DNA interaction, it has been found that the complex **3** was more effective when compared to other complexes because of higher K_b and K_{sv} values and circular dichroism spectra.

The inhibition efficiencies of ligands and their nickel(II) complexes were tested against four pathogenic bacteria species (*Staphylococcus aureus*, *Bacillus subtilis*, *Escherichia coli* and *Pseudomonas aeruginosa*)) and two fungal species (*Aspergillus niger* and *Candida albicans*) by Agar disc diffusion method. The solvent DMSO used as control did not show any zone of inhibition [5]. The experimental result shown in Table S2 indicates that all the complexes are having higher inhibition efficiency than the free ligands, which can be explained on the basis of chelate formation [25]. Minimum inhibitory concentrations (MICs) method (Table 3) was also used to determine the antibacterial activity of the synthesized complexes. Ni(II) complex (MIC = 3.25-17.50 µg/mL) has a greater effect than the effect of ligand against bacteria. Also, Ni(II) complex has been found to have high antifungal activity towards *A. niger* (MIC = 8.25-11.5 µg/mL) and *C. albicans* (MIC = 7.50-11.25 µg/mL) fungi as compared to ligands. The lowest MIC values 3.25 µg/mL and 7.50 µg/mL observed for compound **3**, with the bacteria *S. aureus* and fungus *C. Albicans*, respectively being the most sensitive microorganism.

The minimum energy docked pose [26] of nickel(II) complex **1**–**3** (Figure S6) revealed that the complexes snugly fitted into the curve contour of the targeted DNA in the minor groove and is situated within G-C (~13.2Å) region, and slightly bends the DNA in such a way that a part of the planar aromatic Schiff base makes favourable stacking interactions between DNA base pairs and lead to van der Waals interaction and hydrophobic contacts with DNA functional groups that define the groove [27]. The resulting relative

binding energy of docked ligands L^1, L^2, metal complexes **1–3** with DNA were found to be -310.67, -316.77, -247.24, -298.03, and -342.71, respectively, which is also in accordance with our hypothesis that complex **3** is prominent DNA binder than that of other complexes.

The mononuclear nickel(II) complexes with bappz and its Schiff base ligands (L^1 and L^2) were synthesized and characterised. The single crystal X-ray study confirms the structure of ligands L^1, L^2 and complex **1**. The spectral and structural data give evidences for the proposed coordination behaviour and geometries of the synthesized nickel(II) complexes. The electrochemical study reveals that one quasi-reversible redox wave. The nickel ion in the mononuclear complexes has been translocated between two non-equivalent coordinating compartments of a ditopic ligand by varying the pH of the complex solution. All the nickel(II) complexes (**1–3**) show good binding affinity to BSA protein and DNA giving relatively high binding constants in the order **3** > **2** > **1**. The computer-aided molecular docking studies validate the interaction in the minor groove of DNA helix. All the nickel(II) complexes showed good antimicrobial activity than their free ligands.

Supplementary Material

Crystallographic data in CIF format complex **1** have been deposited at the Cambridge Crystallographic Data Centre, CCDC No. 889112. Copies of CIFs are available free of charge from The Director, CCDC, 12 Union Road, Cambridge, CB2 1EZ, UK (fax: -/44-1223-336-033; email: deposit@ccdc.cam.ac.uk or http://www.ccdc.cam.ac.uk). The mass spectrum of complex **2** is given in the supplementary material.

Acknowledgements

The authors gratefully acknowledge the financial support by the Department of Science and Technology, New Delhi (DST-SR/FT/CS-049/2009). The authors also acknowledge the UGC for providing funds under UGC-BSR research fellowships in science.

The authors thank the SAIF Central Drug Research Institute (CDRI), Lucknow for analyzing the mass spectra.

References

[1] (a) C.-L. Liu, M. Wang, T.-L. Zhang, H.-Z. Sun, DNA hydrolysis promoted by di- and multi-nuclear metal complexes, Coord. Chem. Rev. 248 (2004) 147–168. (b) Q. Jiang, N. Xiao, P.-F. Shi, Y.-G. Zhu, Z.-J. Guo, Design of artificial metallonucleases with oxidative mechanism, Coord. Chem. Rev. 251 (2007) 1951– 1972.

[2] C.N. Sudhamani, H.S. Bhojya Naik, T.R. Ravikumar Naik, M.C. Prabhakar, Synthesis, DNA binding and cleavage studies of Ni(II) complexes with fused aromatic N-containing ligands, Spectrochim. Acta A: Mol. Biomol. Spectrosc. 72 (2009) 643–647.

[3] (a) Y.Y. Yu, H.D. Xian, J.F. Liu, G.L. Zhao, Synthesis, characterization, crystal structure and antibacterial activities of transition metal(II) complexes of the schiff base 2-[(4-methylphenylimino)methyl]-6-methoxyphenol, Molecules 14 (2009) 1747–1754. (b) P.G. Cozzi, Metal–salen schiff base complexes in catalysis: practical aspects, Chem. Soc. Rev. 33 (2004) 410–412.

[4] (a) G.B. Bagihalli, S.A. Patil, P.S. Badami, Synthesis, spectral characterization, in vitro microbial and cytotoxic studies of lanthanum(III) and thorium(IV) complexes with 1,2,4-triazole Schiff bases, J. Enzyme Inhib. Med. Chem. 24 (2009) 730–741. (b) M.M. Omar, G.G. Mohamed, A.A. Ibrahim, Spectroscopic characterization of metal complexes of novel Schiff base. Synthesis, thermal and biological activity studies, Spectrochim. Acta A: Mol. Biomol. Spectrosc. 73 (2009) 358–369.

[5] A. Jayamani, V. Thamilarasan, N. Sengottuvelan, P. Manisankar, S. K. Kang, Y.I. Kim, V. Ganesan, Synthesis of mononuclear copper(II) complexes of acyclic Schiff's base ligands: Spectral, structural, electrochemical, antibacterial, DNA binding and cleavage activity, Spectrochim. Acta Part A: Mol. Biomol. Spectrosc. 122 (2014) 365–374.

[6] Synthesis of **1**: To a solution of 1,4-bis(3-aminopropyl) piperazine (0.10 g, 0.49 mM) in methanol (10 mL), $Ni(ClO_4)_2.6H_2O$ (0.19 g, 0.49 mM) in 10 mL of methanol was added drop wise. The mixture was stirred well at room temperature and refluxed for about 2 h resulted in light brown solution. The solution was concentrated, dried and recrystallized in acetonitrile. Pale brown crystals of **1** were formed at the bottom of the vessel by slow evaporation of the solvent after few days. The crystals were isolated by filtration, washed with methanol and dried. Yield: 0.23 g (78%). m.p.: 174 °C (dec). Anal. Calcd. (%) for $C_{10}H_{24}Cl_2NiN_4O_8$: C, 26.23; H, 5.28; N, 12.24. Found (%): C, 26.27; H, 5.24; N, 12.18. FT-IR (ν, cm^{-1}) (KBr disc): 2867m, 2923br, 1630s, 1139s, 625s. λ_{max}, nm (ε, M^{-1} cm^{-1}) in DMF: 623 (520), 384 (12900), 278 (48006).

[7] Synthesis of **2**: To a solution of ligand (L^1) (0.20 g, 0.46 mM) in methanol (10 mL), $Ni(ClO_4)_2.6H_2O$ (0.17 g, 0.46 mM) in 10 mL of methanol was added drop wise. The mixture was stirred well at room temperature and the content was refluxed for about 3 h. The resultant brown solution was then concentrated to one third of its volume and washed well with water, ethanol and ether and dried under vacuum. Yield: 0.27 g (74%). m.p.: 204 °C (dec.) Anal. Calcd. (%) for $C_{26}H_{36}Cl_2NiN_4O_{10}$: C, 44.98; H, 5.23; N, 8.07. Found (%): C, 44.87; H, 5.24; N, 8.12. FT-IR (ν, cm^{-1}) (KBr disc): 3450w, 3010s, 2867m, 2923br, 1630s, 1225w, 1139s, 625s. λ_{max}, nm (ε, M^{-1} cm^{-1}) in DMF: 639 (329), 396 (16005), 322 (16528), 272 (49504); ESI-MS in CH_3CN *m/z* (%): 247.3 (8) $[C_{14}H_{21}N_3O]^+$, 318.3(22) $[C_{18}H_{30}N_4O]^+$, 375.3(10) $[C_{18}H_{28}N_4NiO]^+$, 493.3 (100) $[NiL^1]^+$, 495.3 (40) $[NiL^1 +2H^+]^+$, 694.2(5) $[NiL^1+2ClO_4]^+$.

[8] Synthesis of **3**: The complex **3** was synthesized using the same procedure as complex **2** using ligand L^2 (0.20 g, 0.35 mM) instead of L^1 with $Ni(ClO_4)_2.6H_2O$ (0.13 g, 0.35 mM) in 10 mL of methanol. Yield: 0.23 g (70%). m.p.: 210 °C (dec.). Anal. Calcd. (%) for $C_{24}H_{30}Br_2Cl_2NiN_4O_{10}$: C, 34.99; H, 3.67; N, 6.80. Found (%): C, 34.95; H, 3.74; N, 6.85.

FT-IR (ν, cm^{-1}) (KBr disc): 3425br, 3017m, 2881m, 2958s, 1625s, 1224w, 1100, 626s. λ_{max}, nm (ε, M^{-1} cm^{-1}) in DMF: 667 (76), 385 (9351), 268 (20788).

[9] The X-ray diffraction analysis of the complex **1** was performed on Bruker SMART APEX-II CCD diffractometer using graphite monochromated MoKα radiation (0.71037Å). The structure was solved using the direct methods and successive Fourier difference synthesis thermal parameters for all non-hydrogen atoms (SHELXL-97) and all non-hydrogen atoms were refined anisotrophically by full-matrix least-square procedures. Hydrogen atoms were added theoretically and refined with riding model position parameters and fixed by isotropic thermal parameters.

[10] S.S. Massoud, F.A. Mautner, Synthesis, characterization, and crystal structure of 1,4-bis(3-aminopropyl)piperazineperchloratocopper(II) perchlorate, Inorg. Chem. Commun. 7 (2004) 559–562.

[11] (a) M.N. Potenza, J.A. Potenza, H.J. Schugar, Structure of tetrakis(1,2-dimethylimidazole)MII diperchlorates (MII = Ni, Cu), Acta Cryst. C44 (1988) 1201–1204. (b) T.-H. Lu, T.H. Tahirov, K. Shu, C.-S. Chung, Copper(II) and Nickel(II) Complexes of 4-Methyl-4,7-diazadecane-1,10-diamine, Acta Cryst. C53 (1997) 204–206.

[12] B. Dede, I. Ozmen, F. Karipcin, Synthesis, characterization, catalase functions and DNA cleavage studies of new homo and heteronuclear Schiff base copper(II) complexes, Polyhedron 28 (2009) 3967–3974.

[13] M. Thirumavalavan, P. Akilan, M. Kandaswamy, Synthesis of lateral macrobicyclic compartmental ligands: structural, magnetic, electrochemical, and catalytic studies of mono and binuclear copper(II) complexes, Inorg. Chem. 42 (2003) 3308–3317.

[14] K.R. Adam, G. Anderegg, L.F. Lindoy, H.C. Lip, M. Mcpartlin, J.H. Rea, R.J. Smith, P.A. Tasker, Metal-ion recognition by macrocyclic ligands. Synthetic, thermodynamic,

kinetic, and structural aspects of the interaction of copper(II) with 14- to 17-membered cyclic ligands containing an O_2N_2-donor set, Inorg. Chem. 19 (1980) 2956–2964.

[15] R. Cao, Q. Shi, D. Sun, M. Hong, W. Bi, Y. Zhao, Syntheses and characterizations of copper(II) polymeric complexes constructed from 1,2,4,5-benzenetetracarboxylic acid, Inorg. Chem. 41 (2002) 6161–6168.

[16] K.-Y. Choi, Synthesis, properties and X-ray crystal structures of nickel(II) complexes of a hexaazamacrotetracyclic ligand, J. Coord. Chem. 56 (2003) 481–491.

[17] M.J. Ettinger, in: D.R. Lontine (Eds.), Copper proteins and copper enzymes, CRC, Boca Raton, FL, 1984, pp. 175–229.

[18] J. Manonmani, R. Thirumurugan, M. Kandaswamy, M. Kuppayee, S. Shanmuga Sundara Raj, M.N. Ponnuswamy, G. Shanmugam, H.K. Fun, Synthesis of mononuclear nickel(II) and copper(II) complexes using compartmental ligands: X-ray and electrochemical studies, Polyhedron 19 (2000) 2011–2018.

[19] (a) Y. Wang, H. Zhang, G. Zhang, W. Tao, S. Tang, Interaction of the flavonoid hesperidin with bovine serum albumin: A fluorescence quenching study, J. Luminescence 126 (2007) 211–218. (b) V. Rajendiran, R. Karthik, M. Palaniandavar, H. Stoeckli-Evans, V.S. Periasamy, M.A. Akbarsha, B.S. Srinag, H. Krishnamurthy, Mixed-ligand copper(II)-phenolate complexes: Effect of coligand on enhanced DNA and protein binding, DNA cleavage, and anticancer activity, Inorg. Chem. 46 (2007) 8208–8221.

[20] A. Tarushi, E. Polatoglou, J. Kljun, I. Turel, G. Psomas, D.P. Kessissoglou, Interaction of Zn(II) with quinolone drugs: Structure and biological evaluation, Dalton Trans. 40 (2011) 9461–9473.

[21] S. Tsiliou, L.-A. Kefala, F. Perdih, I. Turel, D.P. Kessissoglou, G. Psomas, Cobalt(II) complexes with non-steroidal anti-inflammatory drug tolfenamic acid: Structure and biological evaluation, Eur. J. Med. Chem. 48 (2012) 132–142.

[22] R. Prabu, A. Vijayaraj, R. Suresh, L. Jagadish, V. Kaviyarasan, V. Narayanan, New unsymmetric dinuclear copper(II) complexes of trans-disubstituted cyclam derivatives: spectral, electrochemical, magnetic, catalytic, antimicrobial, DNA binding and cleavage studies, Bull. Korean Chem. Soc. 32 (2011) 1669–1678.

[23] E.J. Gao, L. Wang, M.C. Zhu, L. Liu, W.Z. Zhang, Synthesis, characterization, interaction with DNA and cytotoxicity in vitro of the complexes [M(dmphen)(CO3)]·H2O [M = Pt(II), Pd(II)], Eur. J. Med. Chem. 45 (2010) 311–316.

[24] (a) E. Nyarko, N. Hanada, A. Habib, M. Tabata, Fluorescence and phosphorescence spectra of Au(III), Pt(II) and Pd(II) porphyrins with DNA at room temperature, Inorg. Chim. Acta 357 (2004) 739–745. (b) Y. Zhao, J. Zhu, W. He, Z. Yang, Y. Zhu, Y. Li, J. Zhang, Z. Guo, Oxidative DNA Cleavage Promoted by Multinuclear Copper Complexes: Activity Dependence on the Complex Structure, Chem. Eur. J. 12 (2006) 6621–6629.

[25] (a) C.T. Yang, B. Moubaraki, K.S. Murray, J.J. Vittal, Synthesis, characterization and properties of ternary copper(II) complexes containing reduced schiff base N-(2-hydroxybenzyl)-α-amino acids and 1,10-phenanthroline, Dalton Trans. (2003) 880–889. (b) C. Dendrinou-Samara, G. Psomas, C.P. Raptopoulou, D.P. Kessissoglou, Copper(II) complexes with phenoxyalkanoic acids and nitrogen donor heterocyclic ligands: structure and bioactivity, J. Inorg. Biochem. 83 (2001) 7–16.

[26] Molecular docking: The rigid molecular docking studies were performed using HEX 8.0 software. The coordinates of complexes **1** was taken from its respective crystal structure as a CIF file and was converted to the PDB format using Mercury software (http://www.ccdc.cam.ac.uk/). However, structure of the complexes **2** and **3** were sketched by CHEMSKETCH (http://www.acdlabs.com) and converted to PDB format from mol format by CHEMDRAW ULTRA 8.0 (http://scistore.cambridgesoft.com/chemdraw). The crystal structure of the B-DNA

dodecamer d(CGCGAATTCGCG)$_2$ (PDB ID: 1BNA) was downloaded from the protein data bank (http://www.rcsb.org./pdb). All calculations were carried out on an Intel Pentium 4, 2.4 GHz based machine running MS Windows XP SP2 as operating system. Visualization of the docked pose has been carried out using CHIMERA (www.cgl.ucsf.edu/chimera).

[27] (a) V. Kettmann, D. Kostalova, H.D. Holtje, Human topoisomerase I poisoning: docking protoberberines into a structure-based binding site model, J. Comput. Aided Mol. Des. 18 (2004) 785–796. (b) S. Tabassum, A. Asim, F. Arjmand, M. Afzal, V. Bagchi, Synthesis and characterization of copper(II) and zinc(II)-based potential chemotherapeutic compounds: Their biological evaluation viz. DNA binding profile, cleavage and antimicrobial activity, Eur. J. Med. Chem. 58 (2012) 308–316.

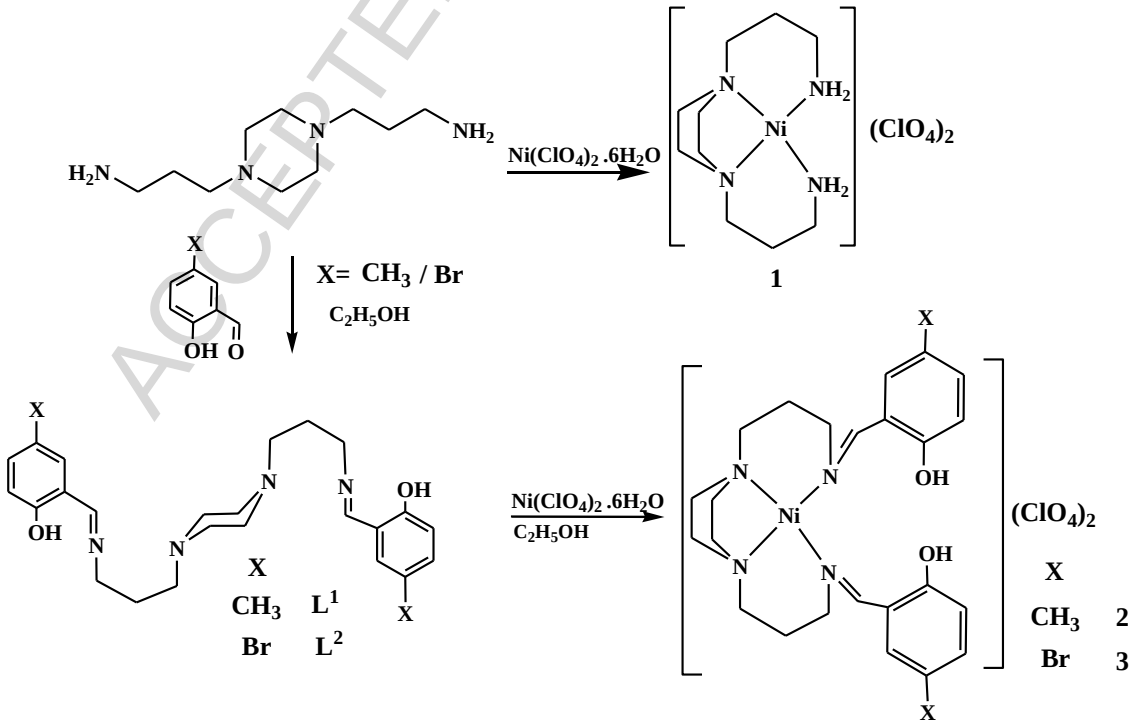

Scheme 1

Figure captions

Figure 1 OPTEP view of the molecular structure and atom labeling scheme of complex **1**

Figure 2 Crystal packing diagram of complex **1**

Figure 3 Plot of % relative fluorescence intensity at λ_{em} = 343 nm (I/I_0%) vs r (r = [compound]/[BSA]) for ligands and their Ni(II) complexes **1**–**3** in buffer solution (150 mM NaCl and 15 mM trisodium citrate at pH 7.0)

Figure 4 Absorption spectra of complex **3** (10^{-5} M) in 5 mM Tris–HCl/20mM NaCl buffer at pH 7.2 in the absence and presence of increasing amounts of DNA. Inset shows the least-squares fit of [DNA]/ε_a-ε_f vs. [DNA] for the complex.

Figure 5 (a) Emission spectra of EB bound to DNA in the presence of nickel(II) complex **3** ([EB] = 3.3 μM, [DNA] = 40 μM, [complex] = 0–25 μM, λ_{ex} = 510 nm). Inset shows the plots of emission intensity I_0/I vs [DNA]/[complex]. (b) Plot of EB relative fluorescence intensity at λ_{em} = 596 nm (I/I_0 (%)) vs r (r = [compound]/[DNA]) for Ni(II) complexes **1–3** in buffer solution (5 mM NaCl and 5 mM Tris–HCl at pH 7.4).

Figure 6 Circular dichroism spectra of CT-DNA (10×10^{-5} M) in Tris–HCl (5 mM) (pH7.2) in the presence of increasing amounts of nickel complexes **1–3** (5×10^{-5} M).

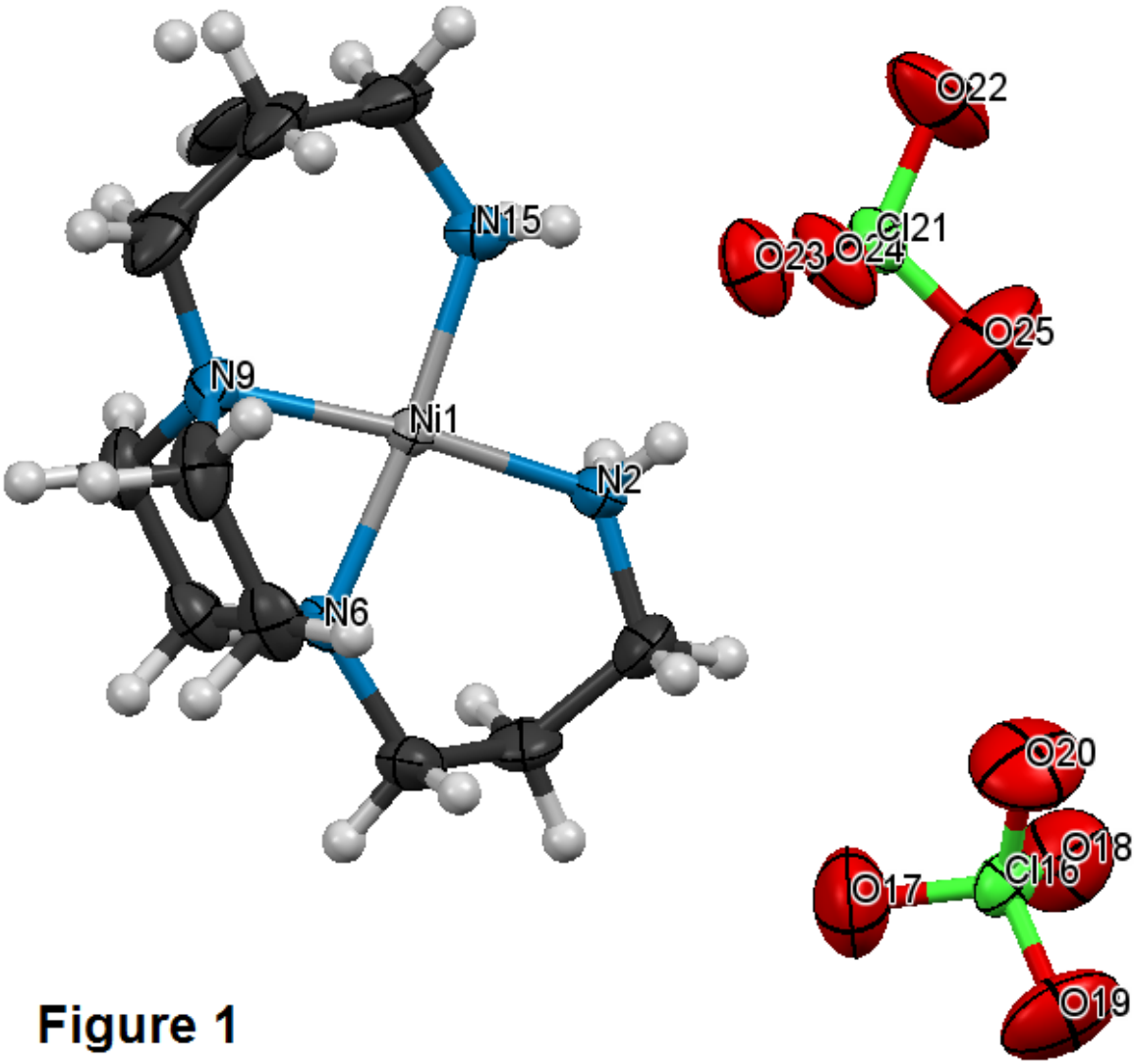

Figure 1

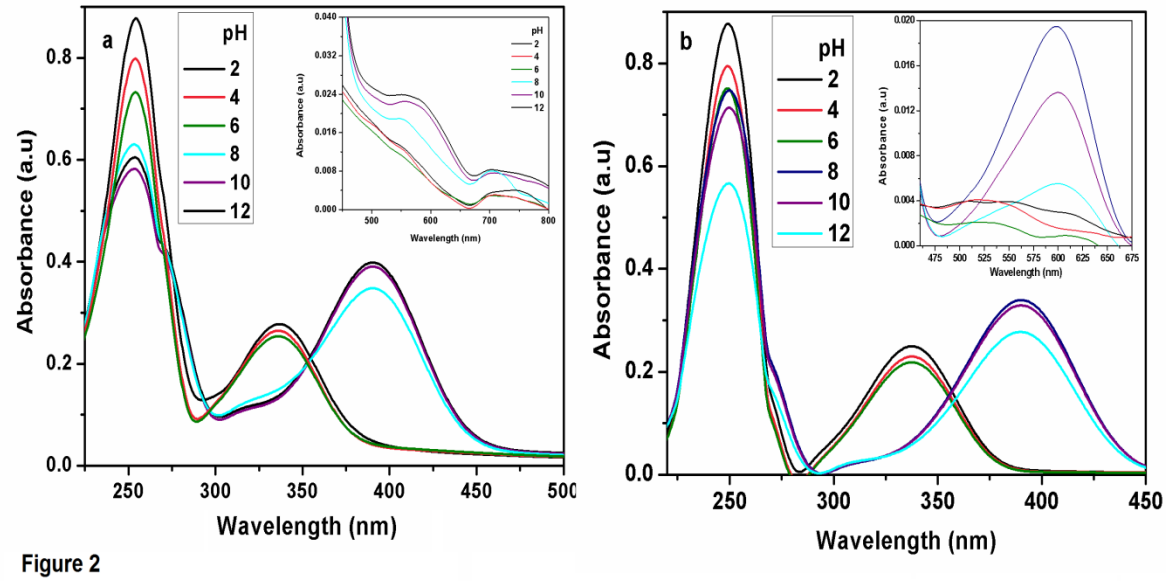

Figure 2

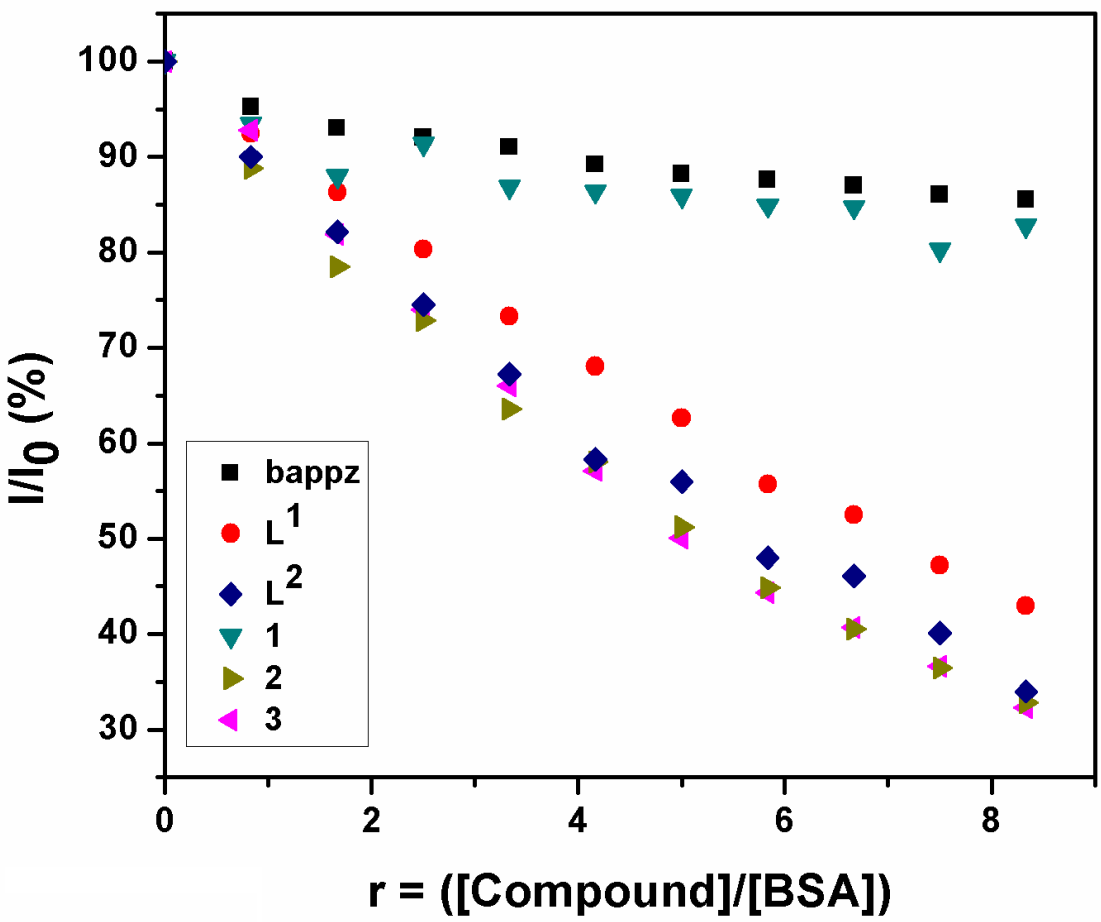

Figure 3

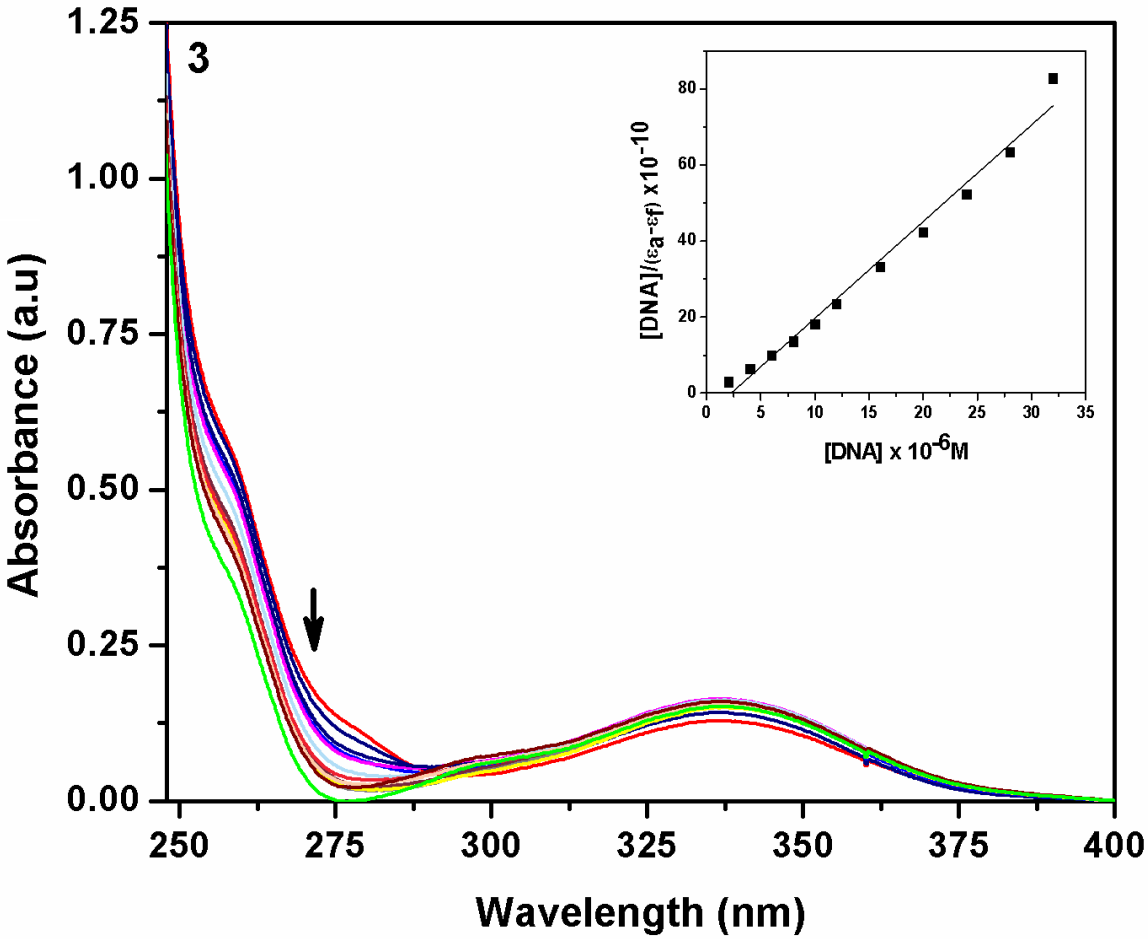

Figure 4

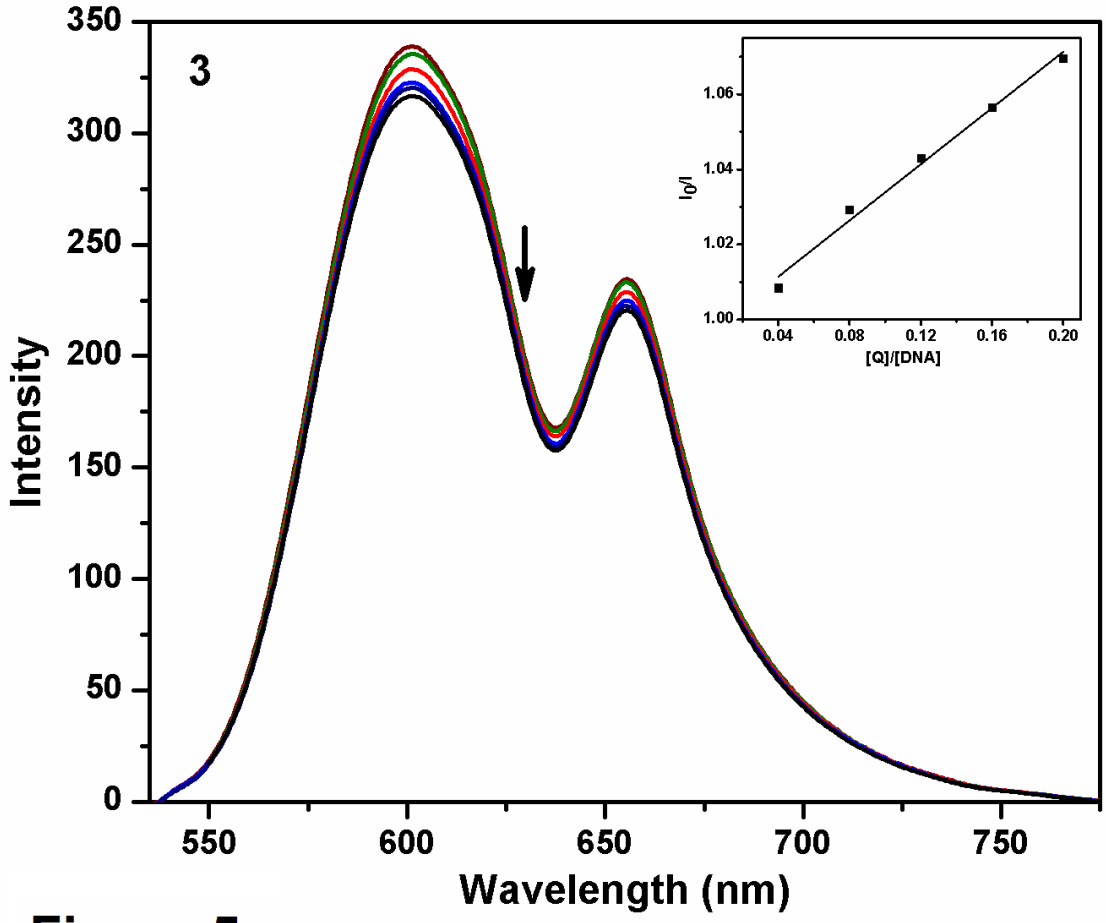

Figure 5a

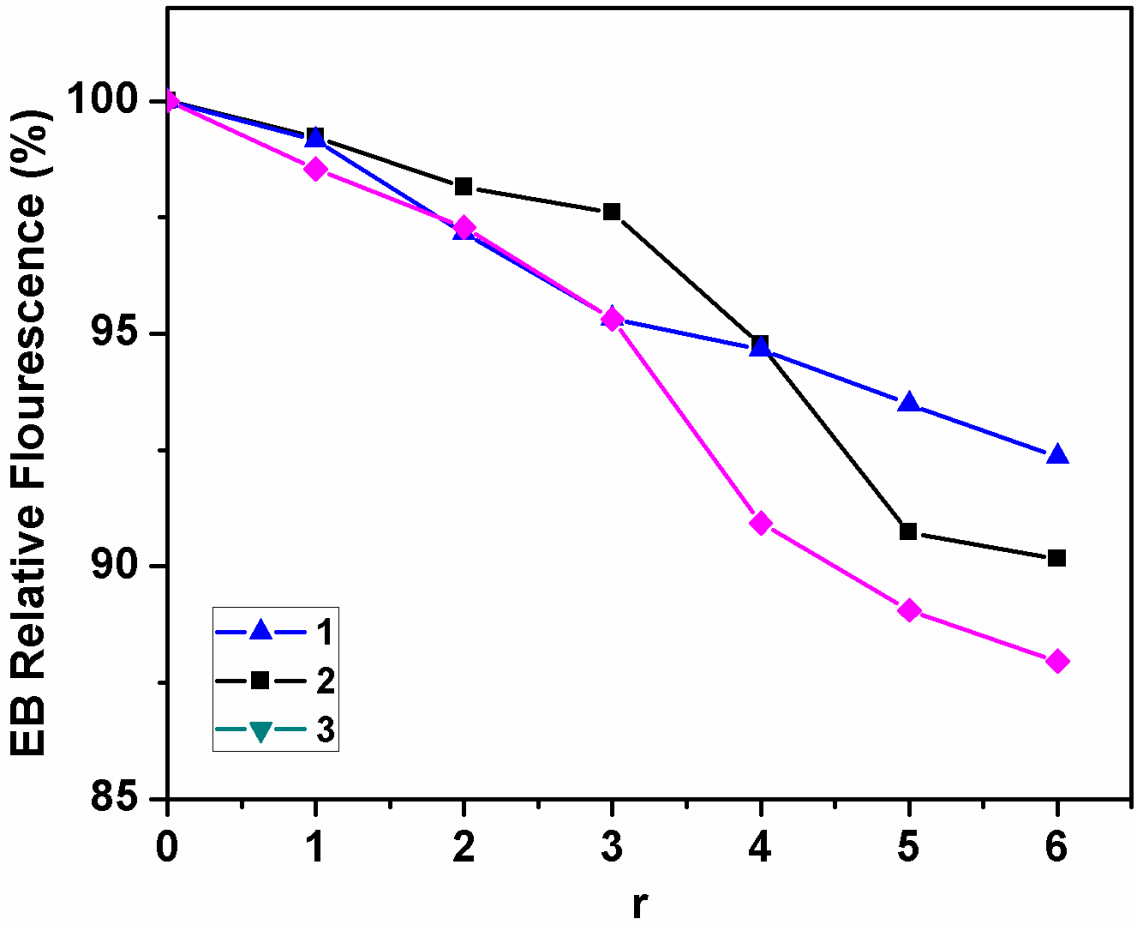

Figure 5b

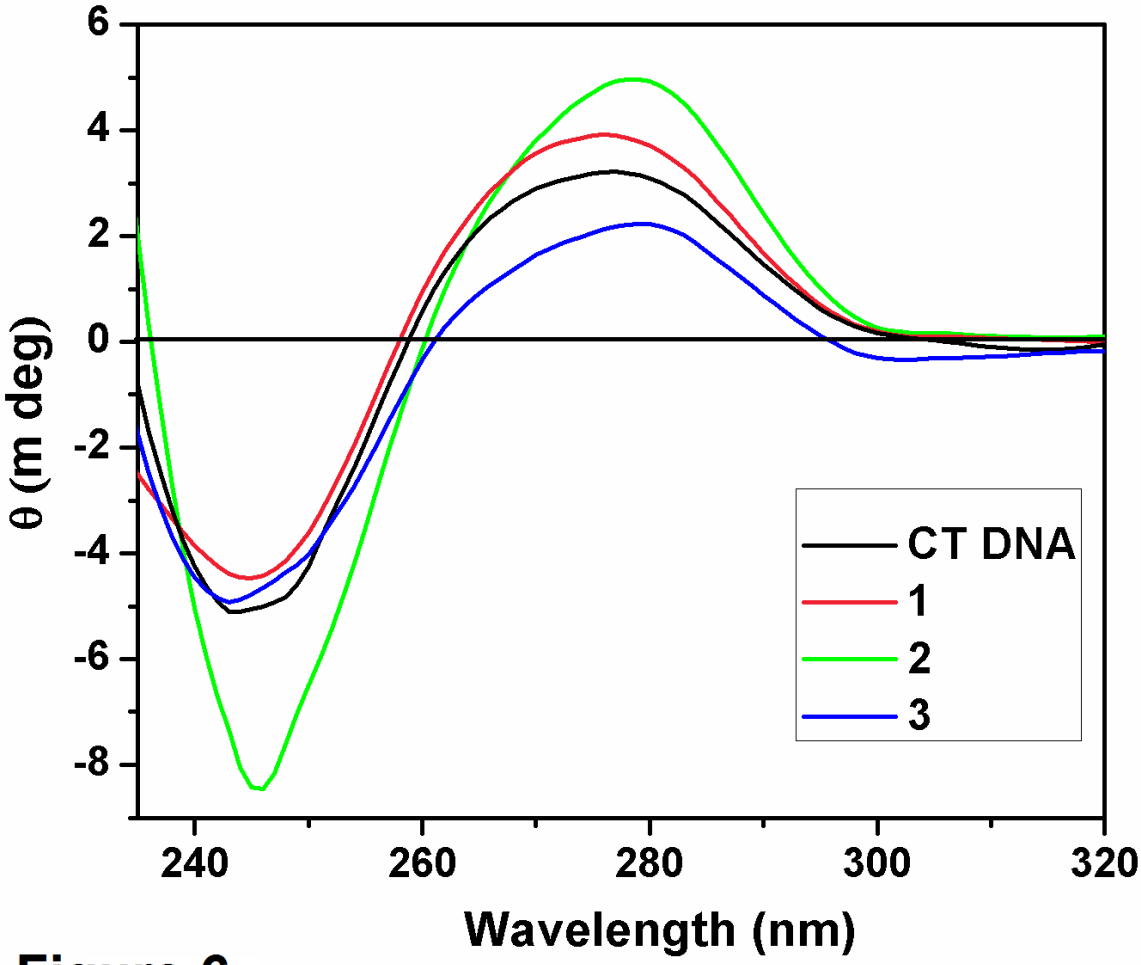

Figure 6

Table 1. Crystallographic data and structure refinement parameters for complex **1**

	1
Empirical formula	$C_{10}\ H_{24}\ Cl_2\ N_4\ Ni\ O_8$
Formula weight	457.94
Temperature (K)	296(2)
Wavelength (Å)	0.71073
Crystal system, space group	orthorhombic, P*bca*
*a (*Å)	14.4352(11)
*B(*Å)	15.4172(12)
c (Å)	16.1779(13)
α (°)	90
β (°)	90
γ (°)	90
Volume (Å^3)	3600.4(5)
Z, calculated density (mg m^{-3})	8, 1.690
Absorption coefficient (mm^{-1})	1.421
F(000)	1904
Crystal size (mm)	0.18 ×0.15 ×0.12
Theta range for data collection (°)	2.31 to 25.50
Limiting indices, *h,k,l*	$-17 \leq h \leq 17$, $-18 \leq k \leq 18$, $-19 \leq l \leq 19$
Reflections collected / unique	21459/3355
*R*int	0.0998
Data / restraints / parameters	3355/ 0 / 234
Goodness-of-fit on F^2	0.819
Final R indices [$I > 2\sigma(I)$]	R1 = 0.0523, wR2 = 0.1272
R indices (all data)	R1 = 0.1158, wR2 = 0.1575
Largest difference peak and hole / e Å^{-3}	0.629 and -0.499

Table 2. The BSA binding constants and parameters (K_{sv}, k_q, K, n) derived for ligands and their Ni(II) complexes (**1**–**3**)

Compound	K_{SV} (M^{-1})	k_q ($M^{-1}s^{-1}$)	K (M^{-1})	n
bappz	5.2 (0.2) x10^3	5.2 (0.2) x10^{11}	1.20 (0.4) x10^5	0.1781
L^1	5.5 (0.6) x10^4	5.5 (0.6) x10^{12}	1.10 (0.2) x10^4	2.65
L^2	7.6 (0.4) x10^4	7.6 (0.4) x10^{12}	1.68 (0.1) x10^4	1.047
1	6.1 (0.1) x10^3	6.1 (0.1) x10^{11}	1.72 (0.1) x10^5	0.222
2	4.5 (0.2) x10^4	4.5 (0.2) x10^{12}	2.1 (0.4) x10^4	2.345
3	8.9 (0.3) x10^4	8.9 (0.03) x10^{12}	9.3 (0.4) x10^4	1.514

Table 3 MIC (μg/ml) of nickel(II) complexes **1**–**3**

Compound	Bacteria				Fungi	
	Gram-negative bacterium		Gram-positive bacterium			
	E.coli	*P.aeruginosa*	*B.subtilis*	*S.aureus*	*A.niger*	*C.albicans*
bappz	>50	>50	>50	>50	>50	>50
L^1	>25	>25	>25	>25	>25	>25
L^2	>25	>25	>25	>25	>25	>25
1	15.00	17.50	10.50	9.50	12.50	11.25
2	12.50	14.50	7.50	6.25	9.50	8.25
3	10.50	12.25	3.25	2.25	8.25	7.50

Graphical abstract

The molecular structure of complex **1** was determined by X-ray crystallography. The nickel ion in the mononuclear complexes has been translocated between two non-equivalent coordinating compartments of ligand by varying the pH. Complexes (**1-3**) were able to bind to DNA and protein in the order **3** > **2** > **1.** Molecular docking studies validated the intercalative mode of binding interaction.

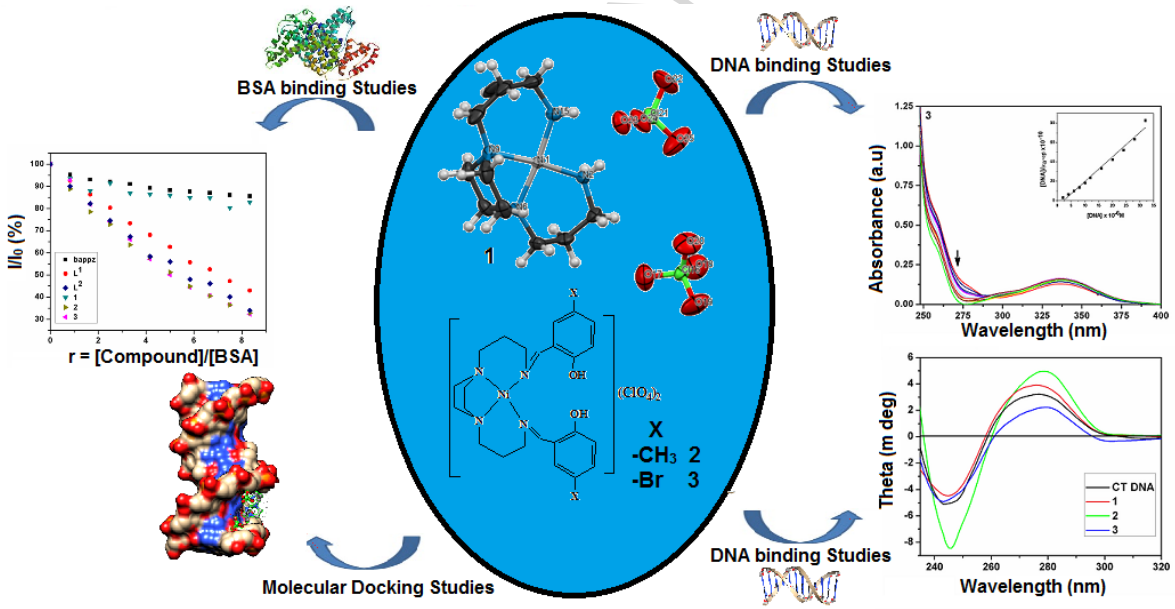

Highlights

- The mononuclear nickel(II) complexes (**1-3**) were synthesized and characterized.
- The molecular structure of complex **1** was determined by X-ray crystallography.
- The position of Ni(II) atom from N_4 to N_2O_2 compartment is achieved by varying pH.
- Complexes (**1-3**) were able to bind to DNA and protein in the order **3**> **2**> **1.**
- The ligands and their nickel(II) complexes exhibited good antimicrobial activity.